

# Prototype of An Optoelectronic Joint Sensor Using Curvature Based Reflector for Body Shape Sensing

Dalia Osman  
Dept. Mechanical &  
Aerospace Engineering  
Brunel University London  
London, UK  
dalia.osman@brunel.ac.uk

Wanlin Li  
The Beijing Institute for  
General Artificial  
Intelligence (BIGAI),  
Beijing, China

Xinli Du  
Dept. Mechanical &  
Aerospace Engineering  
Brunel University  
London  
London, UK

Timothy Minton  
Dept. Mechanical &  
Aerospace Engineering  
Brunel University  
London  
London, UK

Yohan Noh  
Dept. Mechanical &  
Aerospace Engineering  
Brunel University  
London, UK,  
yohan.noh@brunel.ac.uk  
(corresponding author)

**Abstract**—This paper demonstrates a working prototype for shape sensing using miniature optoelectronic sensors integrated into a chain of rotational links. Wearable sensors for rehabilitation, prosthetics and robotics must be lightweight, miniature, and compact to allow comfortable range of motion without obstruction, and therefore, the integrated network of sensors and hardware must be adapted to this. The sensing principle is based on light intensity modulation using a curvature varying reflector. The modular sensing configuration design offers a low-cost, miniaturized approach to shape sensing, compatible in clinical applications. A prototype is constructed, and calibration is carried out. Shape sensing estimation is evaluated to assess accuracy. A four-link rotational chain prototype shows average estimation errors of  $2.4^\circ$  for shape sensing compared to an inertial measurement unit.

**Keywords**—Optoelectronic, shape sensing, wearable device

## I. INTRODUCTION

Wearable technology for monitoring the orientations, shapes, and motion patterns of human joints has emerged in health applications for robotic prosthesis, exosuits, gait analysis, physical therapy, and rehabilitation, as well as areas such as gaming and virtual reality [1]. Integration of sensors within these devices is necessary for accurate position sensing, control, and actuation. Accurate shape sensing in joints of a robotic prosthetic hand for example will allow accurate motion control and can pave the way for integration of haptic feedback for more tactile experience for the user. Sensor systems in worn body joint measurement devices for rehabilitation of patients for post-orthopaedic surgeries or sports therapy, that allow healthcare professionals to track the physical health of body movements, must be of a compact nature, to allow natural unobstructed motion by the user. This miniaturisation of integrated position sensors is challenging, as they must also maintain properties of sufficient sensing range and sensitivity, while allowing flexibility and lightweight of the overall sensing system when integrated into applications such as soft robotics, prosthetics, or joint monitoring devices. Commonly, joint angle measurement sensing is done through the use of optical and magnetic encoders or potentiometers within the context of industrial applications. These can measure joint angle with great precision, although are not practical for use in the mentioned applications for worn sensors, due to large size and weight. For this reason, shape sensing for worn body sensors focuses on flexible or stretchable sensing units, microelectronic sensors, as well as optical based sensing.

Innovative work has been done for angle sensing using film and textile-based sensors. These sensors are incredibly versatile as they are flexible, lightweight, and thin. They are

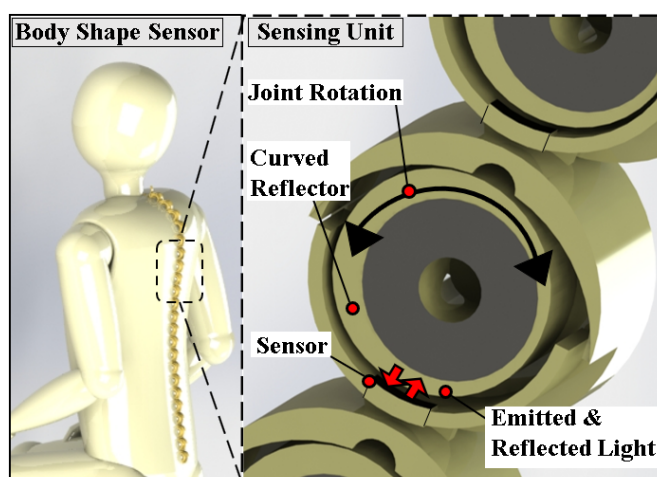


Figure 1: (Left) Concept image for light intensity modulated shape sensing for body joints (adapted from Cults3d, OUDLIDK, 2022). (Right) The optoelectronic sensor is integrated within joint rotational links, opposing a curvature varying reflective surface, that modulates the reflected light intensity during rotation due to proximity difference.

mainly strain based sensors and induce a signal upon resistance change due to deformation of the material. A study in [2] uses an elastic knit fabric coated in a conductive nanocomposite paste and fixed to a frame onto various joints on the body to measure joint angle. Some liquid metal strain gauge stretch sensors have been developed [3][4], where film microchannels are filled with conductive liquids such as *eutectic gallium-indium*. These are used for their fluidity for higher flexibility of sensors, and good conductivity and electrical stability. Some of the downsides however of these types of sensors are eventual wearing down due to prolonged mechanical deformation, and sensing error from signal drift due to the changing of inherent elastic properties over time. Repeated contact exposure to some conductive liquids can also cause irritation over time. Fabrication may also involve multiple complex steps [1]. Flex /strain sensors also display signal non-linearity due to elastic material properties and can be affected by noise due to material inhomogeneity. Lastly, as only stretching is measured, use of this type on sensor as an angle measurement sensor is dependent upon constant geometry from which the sensor is stretched, otherwise precise angle measurement or measurement of complex curves is not possible.

Alternatively, microelectromechanical (MEMS) sensor based wearable motion devices have been used extensively. These components include for example inertial sensors, often used alongside magnetometers, accelerometers, and gyroscopes to measure orientations in multiple axes. These sensors have

been used in simple wearable joint measurement sensors for estimating limb pose by attaching at each joint on the body [5]. Inertial sensors within snake-like robotic manipulators for shape sensing in minimally invasive surgery have also been developed [6]. These MEMs type sensors are smaller in scale and multiple inertial sensors can be integrated along a structure. [7] shows *SensorTape*, a flexible tape with an embedded network of sensors including inertial sensors. Its modular design allows required lengths of tape to be used for shape sensing in three-dimensional space, and can be attached to limbs, suits, and clothing for motion sensing for different applications. One drawback however in the use of inertial sensors is that error can arise during pose estimation due to magnetic interference, gyroscopic drift as well as error from mechanical vibration.

Another type of miniature sensor with potential for use in shape sensing are optical based sensors. An example in [8] is a fibre bragg grating (FBG) based soft wearable system used in upper limb rehabilitation. FBG technology is based on modulating wavelengths of light through gratings that deflect upon change in strain. These gratings are often fused along lengths of optical fibres, and the sensing system can measure a few millimetres in diameter and are incredibly compliant, flexible, and lightweight. Despite this, error in pose estimation can occur under larger deflections in low stiffness conditions [9]. Due to the laborious process of engraving gratings onto optical fibres, making manufacturing difficult, and interrogators for recording the optical signals costing up to thousands of pounds, alternative optical based sensing has been explored. Optoelectronics sensors have been used for pose and joint estimation. These are miniature reflective sensors of a few millimetres in size and comprise of a light emitting diode (LED) and receiving component such as a photodiode or phototransistor, and so can easily be integrated into flexible or soft materials as part of a shape sensing system. An example of use shown in [10] is a multi-segmented exoskeleton for hand rehabilitation along which optoelectronic sensors were fitted. Light reflected from each consecutive segment of the exoskeleton was measured by the optoelectronic sensors and used to estimate overall angle of the bending section. Results of these studies showed sensing range of 90° using multiple sensors. As such, despite use of these miniature sensors, the configuration meant that many sensors were required for this range.

Considering alternative optoelectronic sensing configurations, preliminary studies of a variable curvature reflective surface with optoelectronics were previously used for joint estimation [11], and this study forms the basis of the work demonstrated in this paper. This preliminary work demonstrated a miniature joint estimation technique based on modulation of reflected light intensity using a reflective curved surface coupled axially with a joint housing an optoelectronic sensor that opposed the reflective surface, to induce a varying voltage signal with rotation, to be used to estimate joint angle. As shown in Figure 1, this principle is illustrated. This previous work investigated this principle and how the sensing performance could be improved in terms of sensitivity, range, and accuracy by optimising the curvature variation of the reflective surface. In this paper, this idea will be carried forward by developing a prototype of a chain-link manipulator inte-

grating this optoelectronic sensing principle to test the feasibility of application into wearable soft or flexible shape sensing applications. By continuing to use the miniature optoelectronics sensor - the NJL5901R-2 (New Japan Radio Photodetector, 1.0x1.4x0.6 mm<sup>3</sup>), the sensing configuration can be reduced in size, along with the short distance range responsiveness of this chosen sensor (0-2 mm) which enables this feature of miniaturisation, contrasting to earlier models of sensors used in joint position sensing such as the QRE1113 [12]. The compact nature of the sensing configuration means it can be integrated into small rotational links and allows versatile application due to the essentially modular design, so can be tailored to required lengths for particular applications. As such, this results in a narrow and flexible shape sensing tool for application into wearable devices for physical limb rehabilitation, prosthetic robots, as well as haptic gloves, or exosuits in health as well as gaming and VR to measure complex curvatures in one plane. In terms of safety and compatibility in human application, the sensor features low power consumption, and does not exhibit signal disturbance due to magnetic, material, or electrical interference from other devices. The optics-based method ensures fast sampling rate, and the sensor cost is low (£0.20/unit), resulting in reduced cost of fabrication. Through design of a prototype, calibration of each sensor along the chain links will be carried out, so that the joint angles and overall shape of the chain manipulator can be estimated and evaluated.

## II. THEORETICAL BACKGROUND

### A. Sensing Principle

As mentioned previously, the principle of sensing using the optoelectronic sensors for joint angle measurement is based on the intensity modulation of reflected light, based on proximity to a reflected surface. Comprising of an LED and Phototransistor, the optoelectronic sensor can emit and detect infrared light. In reference to earlier work [11], a light intensity model was derived in order to predicted behaviour of light collected by the phototransistor based on different curved reflecting surfaces rather than flat reflective surfaces. This was a gaussian based intensity model, predicting the cross-sectional flux  $\phi_c$  collected through the phototransistor (Eq 1), before converting to a theoretical voltage value  $V_{th}$  (Eq 2). It was shown that by altering the curvature of this reflector, the flux collected by the phototransistor could be altered to vary the signal voltage variation over a given angular range. By designing a reflector that was steeper, or of higher curvature, the voltage variation of the sensor could be increased over a given joint angle range. As such, the resolution, or sensing sensitivity of the sensing system could be altered, for improved accuracy of specialised application, depending on the required sensing range. This fact was supported by experimental data collected from testing surfaces of various curvatures.

$$\phi_c = \int_{-\frac{3}{2}d - \epsilon}^{-\frac{1}{2}d - \epsilon} \int_{-\sqrt{\left(\frac{d}{2}\right)^2 - (y - h \tan(\theta) + d + \epsilon)^2}}^{\sqrt{\left(\frac{d}{2}\right)^2 - (y - h \tan(\theta) + d + \epsilon)^2}} I_0 e^{-2\left(\frac{x^2 + y^2}{a^2}\right)} dy dx \quad (1)$$

$$V_{th} = \phi_c \cdot R \cdot k_v \quad (2)$$

### III. METHODS & MATERIALS

#### A. Prototype Design

Based on this work, a prototype of a rigid link chain integrated with the sensing system is developed. To do this, each link comprised of the curved reflecting surface. Set over a range of  $140^\circ$ , the thickness of the reflector changes over a 2mm range, shown in Figure 2. This is in line with the sensor responsive range in reference to the sensor's technical data sheet, as mentioned in previous work [13], and so proximity between the sensor and the curve will increase as rotation ensues, resulting in a varying voltage signal. The full prototype is seen in Figure 3, consisting of 30mm disk joints linked together using rotational bearings. A varying curvature-based surface reflector is designed as part of the rotational joint, with a 47mm distance between each link.

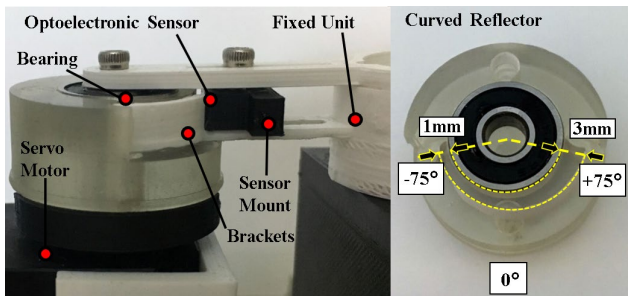


Figure 2: (Left) Experimental platform for carrying out calibration of each sensing unit in link chain. Rotating unit is attached to motor horn, while sensor is mounted onto sensor sliding component of the fixed unit. (Right) Curved surface reflector parameters

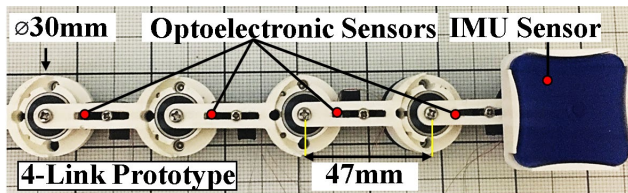


Figure 3: Testing prototype using 4 links coupled using bearings to form one degree of freedom chain, housing curvature based optoelectronic sensing within each joint.

#### B. Calibration Set-up

To evaluate the performance of the sensing system described, a prototype of a link chain manipulator was constructed comprising of units rotating in one degree of freedom. Each unit has the specially designed curve reflector as part of its structure. The optoelectronic sensor is fixed within a channel along the joining link on a sensor mount that can slide along the link and allows optimisation of sensor placement. The joint link also consists of a bracket used to block some external ambient light source. Bearings are used at each joint to allow rotational motion between the units. To calibrate each sensor, the testing set up as shown in Figure 2 was used. Here, a DC Servo Motor (Dynamixel XL-430-W-250T, ROBOTIS, South Korea) was used to generate rotational motion. Each optoelectronic sensor was calibrated individually by mounting the disk of one link to the motor horn, with the coupled link fixed onto an adjacent fixture. In this way, the sensor was fixed within the link, and the coupled unit is able to rotate with the motor. All components were designed using CAD

and 3D printed using PLA (Polylactic acid) plastic material. The curved surface reflector area was coloured white for higher reflectivity. The sensors were wired to an Arduino Mega ADK board (5V). The Dynamixel Motor was powered using a 12V supply and connected to a PC using a U2D2 communication USB device. Developed python interface software was used to synchronously send motor position commands and record analogue sensor data along with motor encoder position data. From this, angular range data was known. Hence, each sensor, and coupled link unit was fixed onto the testing rig, where the motor was rotated through a set angular range, while the sensor signal was recorded. Using the motor encoder position as ground truth, a fifth order linear polynomial regression model was used to map the sensor values. Equation 3 shows this model for link angle estimation using the coefficients  $C_1$  to  $C_5$ , multiplied by the sensor value  $v$  for that link. Results of this calibration are shown in the following section.

$$\theta_i = C_1 v_i^5 + C_2 v_i^4 + C_3 v_i^3 + C_4 v_i^2 + C_5 v_i + C_6 \quad (3)$$

$$x_i = x_{i-1} + l_i \cos(\theta_i + \theta_{i-1}) \quad (4)$$

$$y_i = y_{i-1} + l_i \sin(\theta_i + \theta_{i-1}) \quad (5)$$

where  $i = 1, 2, 3, 4$

$$\theta_{final} = \theta_1 + \theta_2 + \theta_3 + \theta_4 \quad (6)$$

Once all the sensors were calibrated, the next tests were used to evaluate the sensing performance. Here, a range of shapes were constructed using the chain of links of the prototype structure shown in Figure 3. An inertial measurement unit (IMU)(LPMS-B2, LP-Research) sensor was fixed to the end link, to read ground truth angular values of the final link, while all sensor data was simultaneously recorded. The sensor data along with the calibration coefficients were used to estimate the final link angle using a simple rigid link model. Equations (4) and (5) show link position coordinates  $x$  and  $y$ , using link length  $l$  and joint angle estimation  $\theta$  for each link with the initial link grounded. Equation (6) describes the overall angle of the final link as a summation of each estimate. This was compared to the final angle value given by the IMU sensor. Results for this are shown in the following section.

### IV. RESULTS & DISCUSSION

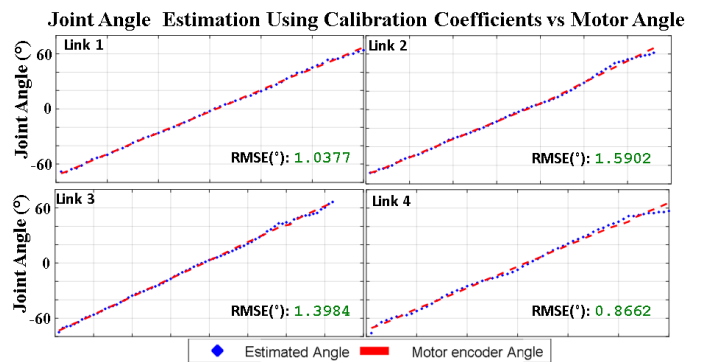


Figure 4: Results of calibrating each of the 4 sensors, using the servo motor encoder data to map the sensor voltage to a joint estimation angle using a linear polynomial regression model. Root Mean Square Error (RMSE) between estimation and true joint angle is shown

## V. CONCLUSION

In conclusion, the proposed miniature optical based joint angle sensing principle based on proximity to a varying curvature reflector has been demonstrated through integration into a one degree of freedom link mechanism, as a prototype to a range of wearable structures upon further miniaturisation. Future steps will include more advanced fabrication techniques for a more specialized prototype for directed wearable or robotic application to be developed and tested under more realistic conditions. Modularisation of the design will allow users to tailor the sensor to their needs, such as certain length or orientation, to be attached onto various surfaces either on the body or various devices.

## ACKNOWLEDGEMENT

This research has received funding from EPSRC DTP, Department of Mechanical and Aerospace Engineering, Brunel University London.

## REFERENCES

- [1] A. I. Faisal, S. Majumder, T. Mondal, D. Cowan, S. Naseh, and M. J. Deen, "Monitoring methods of human body joints: State-of-the-art and research challenges," *Sensors (Switzerland)*, vol. 19, no. 11, Jun. 2019, doi: 10.3390/s19112629.
- [2] M. Xu, J. Qi, F. Li, and Y. Zhang, "Highly stretchable strain sensors with reduced graphene oxide sensing liquids for wearable electronics," *Nanoscale*, vol. 10, no. 11, pp. 5264–5271, 2018.
- [3] S. Kim, J. Lee, and B. Choi, "Stretching and twisting sensing with liquid-metal strain gauges printed on silicone elastomers," *IEEE Sensors Journal*, vol. 15, no. 11, pp. 6077–6078, 2015.
- [4] T. Alam, F. Saidane, A. al Faisal, A. Khan, and G. Hossain, "Smart- textile strain sensor for human joint monitoring," *Sensors and Actuators A: Physical*, vol. 341, Jul. 2022, doi: 10.1016/j.sna.2022.113587.
- [5] T. Lisini Baldi, F. Farina, A. Garulli, A. Giannitrapani, and D. Prattichizzo, "Upper Body Pose Estimation Using Wearable Inertial Sensors and Multiplicative Kalman Filter," *IEEE Sensors Journal*, vol. 20, no. 1, pp. 492–500, Jan. 2020, doi: 10.1109/JSEN.2019.2940612.
- [6] Z. Zhiqiang, Shang Jianzhong, Seneci Carlo, and Yang Guang-Zhong, "Snake Robot Shape Sensing Using Micro-inertial Sensors," Nov. 2013.
- [7] A. Dementyev, H. L. C. Kao, and J. A. Paradiso, "SensorTape: Modular and programmable 3D-aware dense sensor network on a tape," in *UIST 2015 - Proceedings of the 28th Annual ACM Symposium on User Interface Software and Technology*, Nov. 2015, pp. 649–658. doi: 10.1145/2807442.2807507.
- [8] D. lo Presti *et al.*, "A Wearable System Composed of FBG-Based Soft Sensors for Trunk Compensatory Movements Detection in Post-Stroke Hemiplegic Patients," *Sensors*, vol. 22, no. 4, Feb. 2022, doi: 10.3390/s22041386.
- [9] R. Li, Y. Tan, Y. Chen, L. Hong, and Z. Zhou, "Investigation of sensitivity enhancing and temperature compensation for fiber Bragg grating (FBG)-based strain sensor," *Optical Fiber Technology*, vol. 48, no. January, pp. 199–206, 2019.
- [10] B. He *et al.*, "Optoelectronic-Based Pose Sensing for a Hand Rehabilitation Exoskeleton Continuous Structure," *IEEE Sensors Journal*, vol. 22, no. 6, pp. 5606–5615, Mar. 2022.
- [11] D. Osman, W. Li, X. Du, T. Minton, and Y. Noh, "Miniature Optical Joint Measurement Sensor for Robotic Application Using Curvature-Based Reflecting Surfaces," *IEEE Sensors Letters*, vol. 6, no. 5, 2022, doi: 10.1109/LSENS.2022.3169915.
- [12] D. Osman, X. Du, W. Li, and Y. Noh, "An Optical Joint Angle Measurement Sensor based on an Optoelectronic Sensor for Robot Manipulators," *2020 8th International Conference on Control, Mechatronics and Automation, ICCMA 2020*, pp. 28–32, 2020.
- [13] D. Osman, X. Du, W. Li, and Y. Noh, "Development of an Optical Shape Sensing Method Using Optoelectronic Sensors for Soft Flexible Robotic Manipulators in MIS," *IEEE Transactions on Medical Robotics and Bionics*, vol. 4, no. 2, pp. 343–347, May 2022, doi: 10.1109/TMRB.2022.3155200.

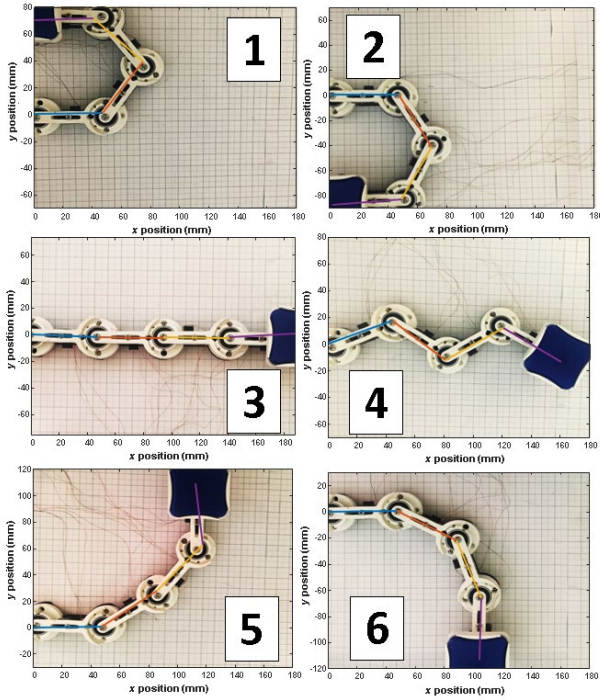


Figure 5.1-6: Shape sensing tests were carried out by constructing varying curvatures and positions of the prototype chain (numbered 1-6) and comparing estimates of final link angle against IMU sensor values. Images of the constructed shapes are graphically overlaid with estimated link angles

TABLE I. 4-LINK SHAPE SENSING RESULTS

Link Shape	Angle Estimation (°)	Actual Angle(°)	RMSE(°)
1	181.78	183.11	1.33
2	-174.94	-177.75	2.81
3	1.21	0.83	0.38
4	-32.72	-30.52	2.20
5	95.10	91.72	3.38
6	-96.06	-91.57	4.31

In reference to Figure 4, showing the fit between the motor encoder angle data and regression model estimates for the calibration experiments of each sensor in the link prototype. In using a fifth-degree polynomial model for fitting, this was able to fit well to the data, with Root Mean Square Error (RMSE) ranging between 0.86 to 1.59°. Following on from this, Figure 5.1-5.6 show the results of the shape sensing test, which included arranging the chain link in varying configurations, and comparing estimated final link angles to that given by the IMU sensor attached at the end of the final link. The shape configurations are imaged, with an overlay of estimated angles for each link. Table 1 shows the percentage error between these two quantities. It can be seen that the shape sensing technique works relatively well and is able to estimate link angles with a degree of accuracy with different constructions of shape, with an overall average root mean square error of 2.40°. To improve upon this, future evaluation will involve development of more specialised application, with the aim of increasing accuracy and miniaturizing the structure.